Journal of Solid State Chemistry **145,** 580–586 (1999)
Article ID jssc.1999.8305, available online at http://www.idealibrary.com on IDEAL®

Dehydration and Rehydration Processes in Microporous Rare-Earth Dicarboxylates: A Study by Thermogravimetry, Thermodiffractometry and Optical Spectroscopy

F. Serpaggi,* T. Luxbacher,*,† A. K. Cheetham,*,‡ and G. Férey*

*Institut Lavoisier, UMR CNRS 173, Université de Versailles Saint-Quentin-en-Yvelines, 45, avenue des Etats-Unis, 78035 Versailles cedex, France; †Institut für Physikalische und Theoretische Chemie, Technische Universität Graz, Rechbauer Strasse 12, 8010 Graz, Austria; and ‡Materials Research Laboratory, University of California at Santa Barbara, Santa Barbara, California 93106

Received January 12, 1999; accepted March 23, 1999

DEDICATED TO PETER DAY ON HIS 60TH BIRTHDAY

The recently discovered microporous materials, $[Ln(H_2O)]_2[O_2C(CH_2)_2CO_2]_3 \cdot H_2O$ and $[Ln_2(H_2O)]_2[O_2C(CH_2)_3CO_2]_3 \cdot 4H_2O$ (Ln = trivalent rare-earth ion), exhibit a three-dimensional organic–inorganic network with channels containing weakly bonded water molecules. The ability of these compounds to reversibly adsorb and desorb these water molecules in the temperature range 25–100°C has been confirmed using thermogravimetry and thermodiffractometry. In addition, the influence of adsorbed water on the lifetime of the $^5D_0$ state of Eu^{3+} has been studied by optical spectroscopy.

INTRODUCTION

The application of zeolites and related microporous materials as drying agents is of great technological interest and many studies on dehydration and rehydration processes in such materials have been carried out, e.g., by using EXAFS (1), XRD (2), and synchrotron X-ray powder diffraction (3). In our search for new microporous materials, we have recently prepared the first open-framework lanthanide succinates, $[Ln(H_2O)]_2[O_2C(CH_2)_2CO_2]_3 \cdot H_2O$, and lanthanide glutarates, $[Ln_2(H_2O)]_2[O_2C(CH_2)_3CO_2]_3 \cdot 4H_2O$ (Ln = trivalent rare-earth ion) (4). Each family of compounds appears to be isostructural for all Ln. Their structures show an organic–inorganic network consisting of chains of edge-sharing $LnO_8(H_2O)$ polyhedra linked together by the carbon chains of the respective dicarboxylic acid along the two perpendicular directions. For both types of compounds, the complex connection leads to channels along the chain direction, and the tunnels contain water molecules which are weakly connected to the carboxylate groups by hydrogen bonds (Figs. 1 and 2). In the glutarate compounds, $[Ln_2(H_2O)]_2[O_2C(CH_2)_3CO_2]_3 \cdot 4H_2O$ hereafter noted Ln[glut], the six water molecules per formula unit belong to two chemically different groups comprising four molecules contained in the channels along the crystallographic a axis and two molecules connected to the rare-earth ions. The stoichiometric ratio of free water molecules (H_2O_{free}): Ln-coordinated molecules (H_2O_{coord}): rare-earth ions is therefore 4:2:2. The channels are smaller in the succinate compounds, $[Ln(H_2O)]_2[O_2C(CH_2)_2CO_2]_3 \cdot H_2O$ (Ln[succ]), because there is one carbon atom less in the dicarboxylate chain. This allows only a single water molecule to be intercalated in the organic framework per cation, so that the corresponding ratio H_2O_{free}: H_2O_{coord}: Ln equals 1:2:2.

In order to determine if these new materials show zeolitic behavior, the loss of water molecules contained in the channels of the lanthanide glutarate and succinate crystals was studied using three independent techniques: thermogravimetric analysis, thermodiffractometry, and rare-earth spectroscopy. Rehydration was also examined. For the spectroscopic study of the dehydration and rehydration processes in these compounds, we have chosen the systems (Eu_xGd_{1-x})[glut] and (Eu_xY_{1-x})[succ] ($x = 0.01$ to $x = 1$). The lowest lying electronic state of Eu^{3+} from which emission can be observed is nondegenerate ($^5D_0$), even at low local symmetries of the surrounding ligands; this is the case in the dicarboxylate crystals. The presence of Eu^{3+} ions at other than the regular lattice sites may therefore easily be detected since the $^7F_0 \leftrightarrow {}^5D_0$ absorption and emission transitions are very sharp ($\leq 2\,cm^{-1}$). Furthermore, since the energy separation to the lower lying $^7F_6$ state spans more than 3 quanta of the highest-energy vibration, multiphonon relaxation processes, which are expected to shorten the lifetime of the $^5D_0$ state efficiently, will take place with minimum probability compared with other rare-earth ions.

0022-4596/99 $30.00

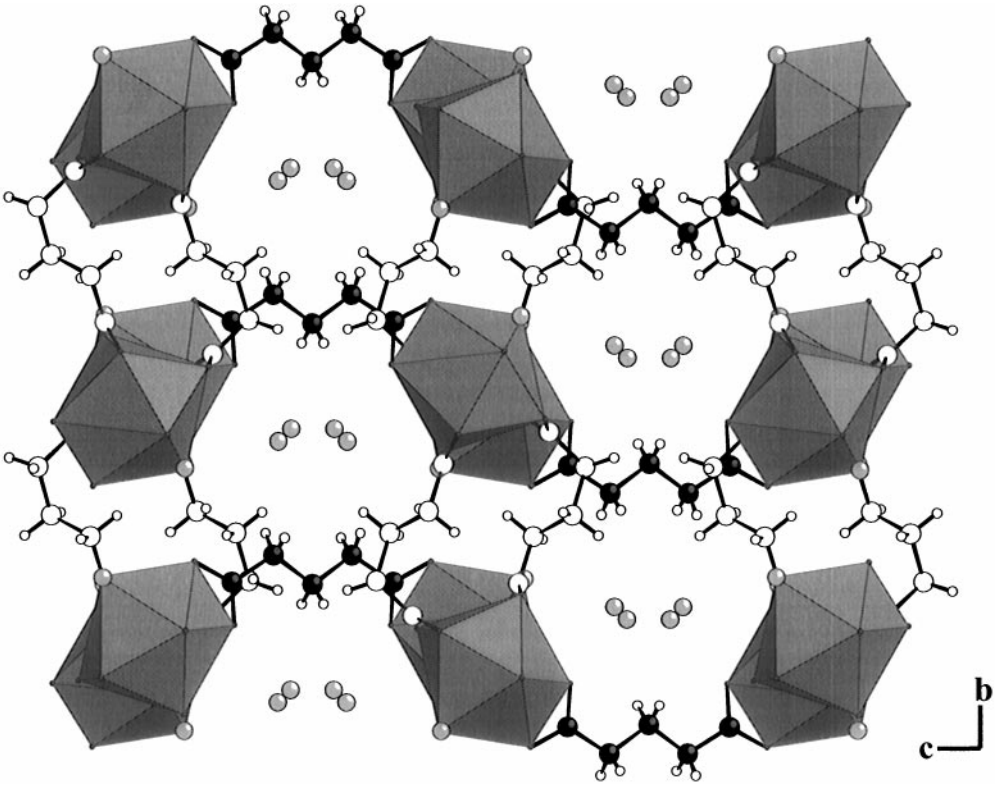

FIG. 1. Projection of the structure of the glutarate, $[Pr(H_2O)]_2[O_2C(CH_2)_3CO_2]_3 \cdot 4H_2O$, along the [100] direction showing four water molecules in the channels and one water molecule per polyhedron (in gray).

EXPERIMENTAL

The rare-earth dicarboxylates were synthesized under hydrothermal conditions (200°C for 3 days) by the reaction of lanthanide chloride with succinic acid, $HO_2C(CH_2)_2CO_2H$, and glutaric acid, $HO_2C(CH_2)_3CO_2H$, respectively (4). Crystals of several lanthanide dicarboxylates were obtained and their structures confirmed by single crystal X-ray diffraction. Samples of (Eu_xGd_{1-x})[glut] and (Eu_xY_{1-x})[succ] with approximated composition $x = 0.01$ (succinate only), 0.05 (glutarate only), 0.10, 0.25, and $x = 1$ were prepared. Chemical analysis gave 5.3%, 10.4%, and 25.8% Eu for the glutarates, and 1.0% 10.4%, and 25.1% for the succinates.

Thermogravimetric analyses were carried out on a TA-Instrument type 2050 thermoanalyzer under O_2 gas flow with a heating rate of $5°C \cdot min^{-1}$ over the temperature range 25–900°C (Fig. 3). For the supplementary TGA curve shown in Fig. 4, the material was heated to 80°C (heating rate: $+1°C \cdot min^{-1}$), kept at 80°C for 2 h, and then cooled to 25°C (cooling rate: $-1°C \cdot min^{-1}$).

Thermodiffractometry measurements were run under ambient air on a Siemens D5000 diffractometer with Co$K\alpha$ radiation in the range $8° < 2\theta < 40°$ with a step size of 0.02° (2θ) and an acquisition time of 20 s per step. The compounds were heated to 80°C (heating rate: $+0.6°C \cdot min^{-1}$), and then cooled to room temperature (cooling rate: $-0.6°C \cdot min^{-1}$). Diagrams were collected every 5°C.

Optical emission spectra were obtained from powder samples under 465.8 nm continuous wave excitation of a Spectra Physics 164 Ar ion laser. The emission was dispersed by a 1 m Jarrell-Ash monochromator and detected by a Hamamatsu R 374 photomultiplier. Low temperature spectra were recorded by immersing the sample in liquid nitrogen in a quartz sample holder.

Luminescence decay curves were observed at $16207 \pm 20\,cm^{-1}$ for the Eu^{3+} $^5D_0 \rightarrow {}^7F_2$ emission after pulsed laser excitation into the Eu^{3+} $^7F_0 \rightarrow {}^5D_0$ transition at $17268 \pm 10\,cm^{-1}$. The measurements were carried out with a Spectron doubled Nd:YAG laser pumping a Spectron dye laser with Rhodamin 6G dissolved in ethanol as the laser dye (pulse duration 7 ns, 10 pulses/s). The emission was dispersed with a 0.22 m monochromator with a $600\,mm^{-1}$ grating and 0.25 mm slits (SPEX minimate) and detected by a cooled C31034A photomultiplier tube. The output from the photomultiplier was amplified by a Stanford Research Systems SR445 preamplifier and the photons counted by a SR430 multichannel Scaler/Averager.

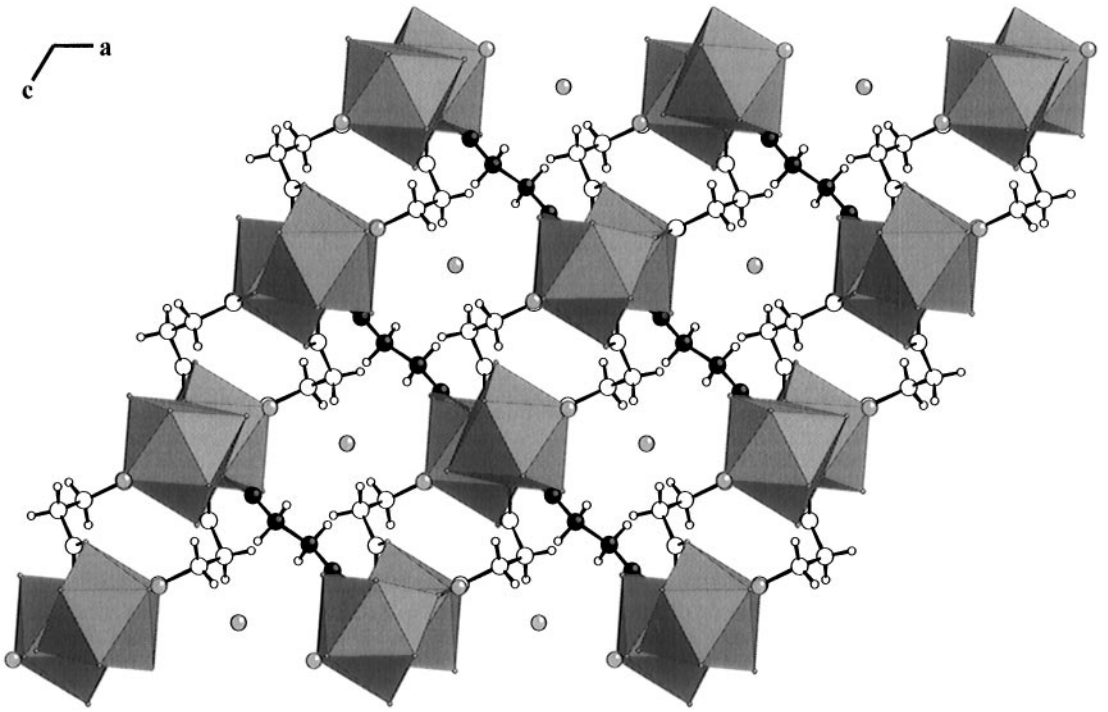

FIG. 2. Projection of the structure of the succinate, $[Pr(H_2O)]_2[O_2C(CH_2)_2CO_2]_3 \cdot H_2O$, along the [010] direction showing one water molecule inside the channels and one water molecule per polyhedron (in gray).

For the measurements, 4 kByte bins each of 1.28 μs width were counted with a maximum count rate of 1 MHz per bin until a maximum of 10,000 to 30,000 counts per bin was accumulated. Actual power levels incident upon the sample were of the order of 100 μJ per pulse in an area of about 4 mm^2. The samples were cooled and heated, respectively, using a laboratory built nitrogen cryostat. The heating rate was approximately the same as in the TGA study shown in Fig. 4; we were unable to measure the water content at each stage during this experiment.

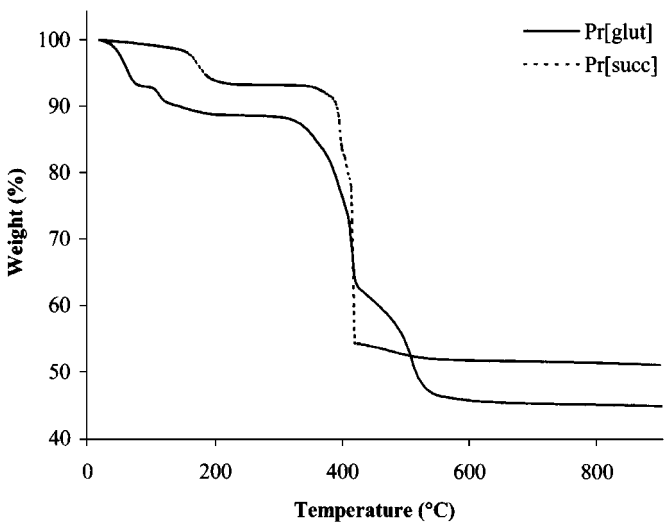

FIG. 3. TGA curves of $[Pr(H_2O)]_2[O_2C(CH_2)_3CO_2]_3 \cdot 4H_2O$ and $[Pr(H_2O)]_2[O_2C(CH_2)_2CO_2]_3 \cdot H_2O$ (dotted line).

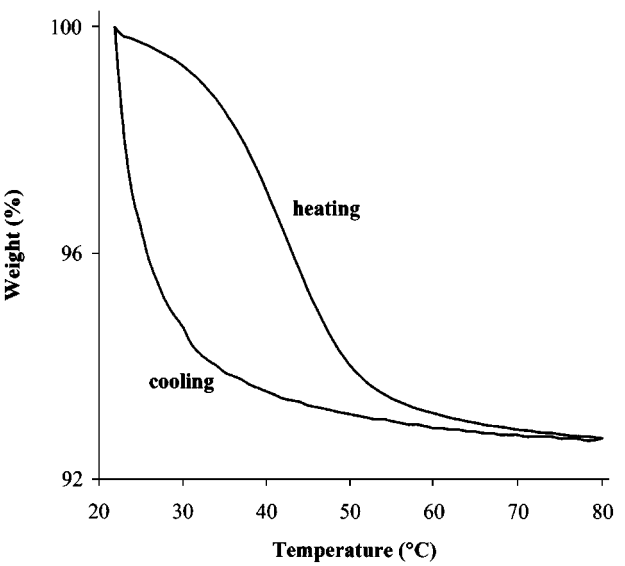

FIG. 4. TGA curve of $[Pr(H_2O)]_2[O_2C(CH_2)_3CO_2]_3 \cdot 4H_2O$ showing the reversible dehydration (loss of weakly bonded water molecules in the channels during heating) and rehydration processes.

RESULTS AND DISCUSSION

Thermogravimetric Analysis

The structure determination of lanthanide glutarate by single crystal X-ray diffraction (4) indicates the general formula $[Ln(H_2O)]_2[O_2C(CH_2)_3CO_2]_3 \cdot 4H_2O$ and shows the presence of two types of water molecules: one third of the water molecules are coordinated to the rare earth cation and the residual water molecules are contained in the channels along the crystallographic *a* axis. This is in agreement with the thermogravimetric analyses which show two successive losses of weight below 320°C. As a representative example, the TGA curve of Pr[glut] is shown in Fig. 3. The first loss (calc., 9.2%; found, 7.8%) corresponds to the departure of the weakly bonded water molecules in the tunnels and occurs between room temperature and ~100°C. The second loss in the range 110–320°C corresponds to the withdrawal of the coordinated water molecules (calc., 4.6%; found, 4.2%). The existence of a plateau of 10°C duration between the two losses allows the selective study of the dehydration and rehydration processes of the compounds. The final loss starting above 320°C corresponds to the decomposition of the organic part of the framework terminating at about 550°C (calc., 42.5%; found, 43.1%). The residual compound was confirmed by X-ray diffraction to be Pr_6O_{11} (5).

The supplementary TGA in the temperature range 25°C to 80°C shows the reversibility of the dehydration and rehydration processes of the glutarate compounds in more detail. The TGA curve for Pr[glut] in Fig. 4 indicates that the compound is losing its free water molecules when heated to 80°C. As the temperature is decreased, the partly dehydrated compound recovers the same amount of the water at almost the same rate with an hysteresis of about15°C. Repeated cycling shows this behavior to be exactly reproducible.

In Fig. 3 the broken line corresponds to the TGA curve for Pr[succ]. The major difference in the thermal behavior of succinates is the loss of water molecules at temperatures below 320°C (calc., 7.9%; found, 6.8%). While for glutarate the chemically different water molecules are withdrawn in two well separated steps, a continuous loss of water is observed for the succinate compounds in the temperature range 25–320°C, the main loss being around 150°C. The final decomposition of the organic part occurs at 400°C giving rise to a very sharp change of weight (calc., 42.3%; found, 42.2%). The final compound is again identified as Pr_6O_{11} (5).

Thermodiffractometry

The thermodiffractograms for Pr[glut] shown in Fig. 5 indicate that the crystallinity of the compound is retained

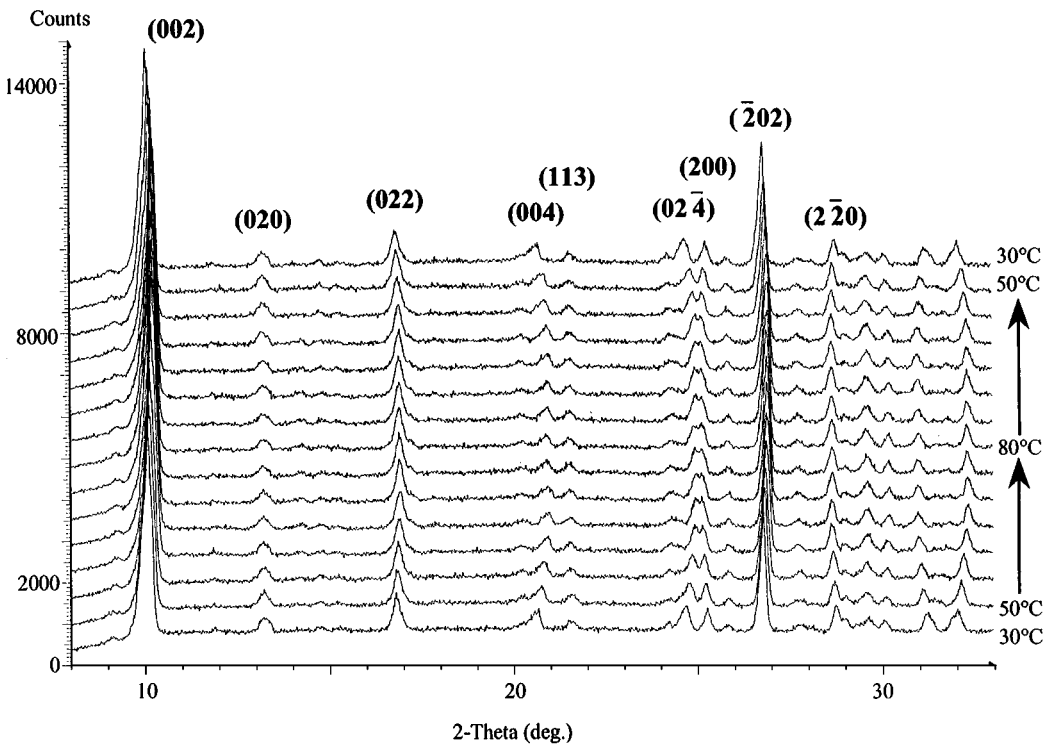

FIG. 5. X-ray thermodiffractometry pattern for $[Pr(H_2O)]_2[O_2C(CH_2)_3CO_2]_3 \cdot 4H_2O$ collected when heating (80°C) and cooling the compound.

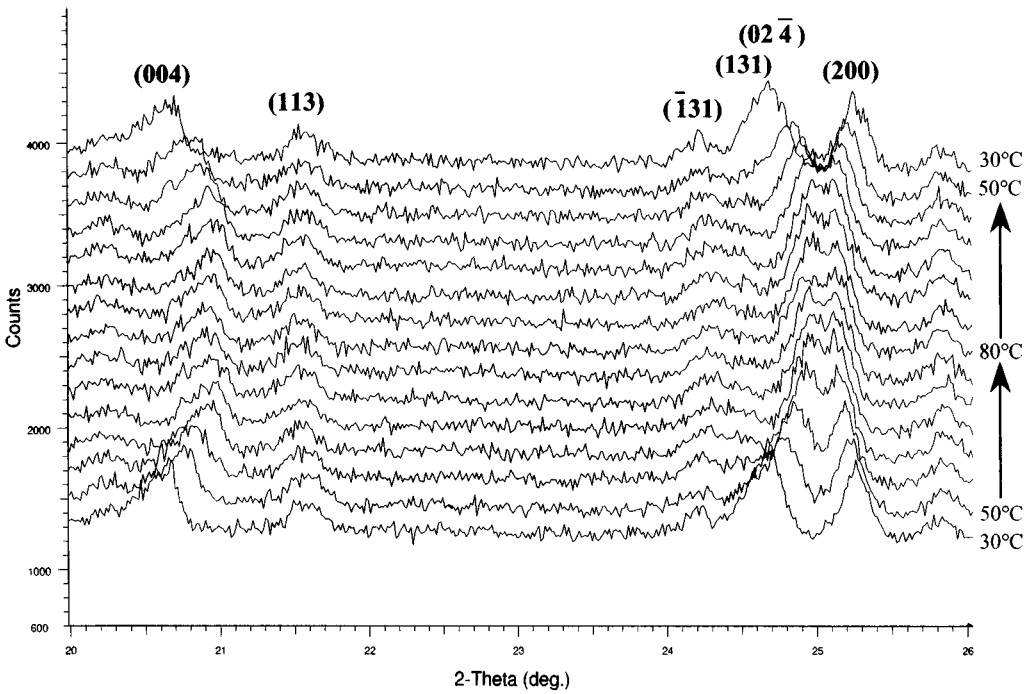

FIG. 6. Detail between 20° and 26° (2θ) of the pattern of Fig. 5 showing the reversibility of both the positions and the intensities of the peaks during the heating/cooling process.

during the heating and cooling processes described in the experimental section. The X-ray patterns in the range 20° to 26° (2θ) are enlarged in Fig. 6 and show reversibility in both the intensities and the positions of the observed lines, confirming the reversibility of dehydration and rehydration of this compound. During heating from 30°C to 80°C, the lines corresponding to the (002), (020), and (200) reflections are slightly shifted by 2θ changes of $+0.13$ deg, -0.01 deg, and -0.09 deg which correspond to d_{hkl} changes of $\Delta d_{002} = -0.14$ Å, $\Delta d_{020} = +0.01$ Å, and $\Delta d_{200} = +0.02$ Å, respectively. Since there is no significant change for d_{200} and d_{020} (corresponding to cell parameters a and b) but a decrease of about 2% in d_{002} (directly related to the cell parameter c), we conclude that the combined effects of heating the compound and the loss of the free water molecules lead to a preferred contraction of the unit cell along the c axis. Indeed, if we draw our attention to Fig. 1, one can imagine that the hydrophobic part of the carboxylate chains (black colored circles) are able to act like springs along the c axis, whereas the lanthanide carboxylate layers assume a higher rigidity.

Rare-Earth Spectroscopy

Figure 7 shows the optical emission spectrum of $(Eu_{0.1}Gd_{0.9})$[glut] in the region of the $^5D_0 \rightarrow {}^7F_J$ ($J = 0, 1, 2$, and 4) transitions at 77°K under continuous Ar ion laser excitation at 465.8 nm. The arrows at about 17,250 cm^{-1} and 16,200 cm^{-1} indicate the transition energies used for resonant excitation and emission detection, respectively, in our lifetime measurements. Very sharp transition lines masked by asterisks are additional lines arising from the spectrum of the Ar ion plasma of the laser.

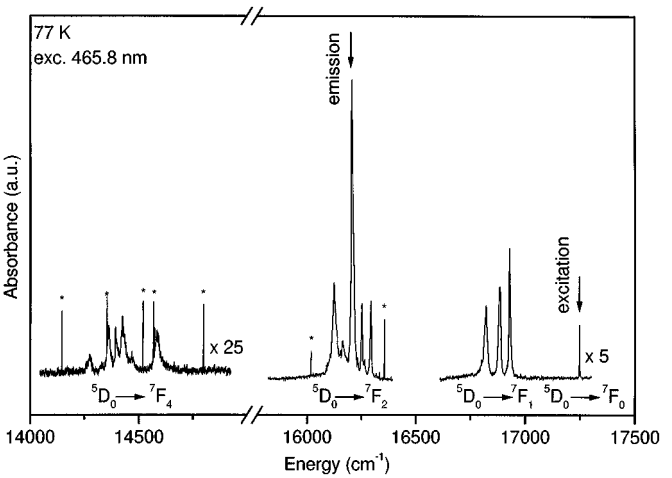

FIG. 7. Optical emission spectrum of $(Eu_{0.1}Gd_{0.9})$[glut] in the region of the $^5D_0 \rightarrow {}^7F_J$ ($J = 0, 1, 2$, and 4) transitions at 77°K under continuous Ar ion laser excitation at 465.8 nm. The arrows at about 17250 cm^{-1} and 16200 cm^{-1} indicate the transition energies used for resonant excitation and emission detection in our lifetime measurements, respectively. Very sharp transition lines masked by asterisks are additional lines arising from the spectrum of the Ar ion plasma of the laser.

At 298° K the luminescent decay of the $^5D_0$ state of Eu^{3+} in $(Eu_{0.01}Gd_{0.99})$[glut] excited resonantly into the $^7F_0 \rightarrow {}^5D_0$ transition at 17268 cm^{-1} and observed for the $^5D_0 \rightarrow {}^7F_2$ transition at 16207 cm^{-1} is strictly exponential over more than 10 half lives with a decay rate of 1711 s^{-1} corresponding to a lifetime of 584 μs. For $0.01 \leq x \leq 1$ no changes in the emission lifetime and the single exponential shape of the decay curves are observed. The absence of concentration quenching of the $^5D_0$ emission may be expected due to the absence of cross-relaxation pathways, but it is not necessarily obligatory. In comparison with the dicarboxylate compounds, europium propylene diphosphonate (6) or the high-symmetry elpasolite crystals $Cs_2NaEu_xGd_{1-x}Cl_6$ (7, 8) and $Cs_2NaEu_xLa_{1-x}(NO_2)_6$ (9) show energy migration in the $^5D_0$ and $^5D_1$ states of Eu^{3+} leading to nonexponential decay curves at concentrations of $x \geq 0.2$.

The distance between nearest-neighbor Eu^{3+} ions in the succinate and glutarate crystals are 4.2 and 4.1 Å, respectively. Efficient energy migration might therefore be expected in these systems. High-frequency vibrations exerted by the intercalated water molecules and the organic framework of these microporous compounds contribute efficiently to the quenching of the $^5D_0$ luminescence and dominate the decay characteristics. If present, energy migration processes are suppressed and not observed under the present experimental conditions.

The evolution of lifetime of the Eu^{3+} $^5D_0$ state in (Eu_xGd_{1-x})[glut] with temperature is shown in Fig. 8. At temperatures below 298°K, the lifetime increases slightly to reach 590 μs at 77°K. This remarkably low change in the lifetime (less than 1%) shows the efficient luminescence quenching due to the presence of free water molecules, even at low temperatures.

At temperatures above 298°K we observe a significant increase in the lifetime of the $^5D_0$ state due to the loss of the intercalated water molecules at 353°K (80°C). The emission decay remains single exponential over the whole concentration range with a rate of $1580 \pm 13\ s^{-1}$ corresponding to a lifetime of 630 ± 5 μs. In the glutarate system, two processes with contrary effects contribute to the temperature dependence of the emission lifetime. Increasing the temperature will decrease the luminescence lifetime due to an increase in the efficiency of multiphonon relaxation. There is also a possibility of thermal population of the $^5D_1$ state from the $^5D_0$ state at higher temperatures, followed by a fast nonradiative decay (10). On the other hand, the loss of two water molecules per rare-earth ion enlarges the emission duration. The combined effects lead to an increase in the lifetime of the $^5D_0$ state of 7.5% compared to the lifetime at 298°K, which correlates nicely with the results of the TGA and thermodiffractometry measurements. The reversibility of the dehydration process is confirmed again since the emission lifetime decreases again after cooling to 298° K, as shown in Fig. 8.

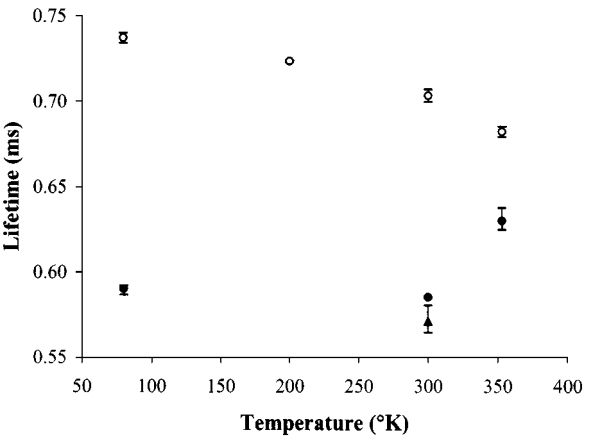

FIG. 8. Temperature evolution of the lifetime of the $^5D_0$ state of Eu^{3+} in $[(Eu_xGd_{1-x})H_2O]_2[O_2C(CH_2)_3CO_2]_3 \cdot 4H_2O$ (●) and $[(Eu_xGd_{1-x})H_2O]_2[O_2C(CH_2)_2CO_2]_3 \cdot H_2O$ (○). The triangle (▲) at 298°K represents the lifetime of the glutarate compound after the dehydration and rehydration process.

For comparison we have studied the decay kinetics of the Eu^{3+} $^5D_0$ state in the succinate system. The luminescence decay curves are again strictly exponential over the whole concentration and temperature ranges studied. At 298° K the lifetime of the $^5D_0$ state is 704 ± 4 μs and therefore significantly higher than in the glutarate system. Decreasing the temperature results in a more pronounced change in the lifetime (−4.5% at 77° K). We ascribe the difference between the glutarate and succinate systems in both the lifetime of the $^5D_0$ state and its evolution with temperature to the smaller number of water molecules in the latter compounds.

The dehydration experiment was performed on the succinate system under the same conditions applied to the glutarate compound. As the temperature is raised, the lifetime continues fall, reaching 682 ± 3 μs at 353°K and showing complete reversibility after cooling. As is shown from the TGA measurements, the loss of half a water molecule per rare-earth ion intercalated in the succinate framework occurs at temperatures well above 373°K and is therefore not detected in the temperature range used in our spectroscopic studies.

CONCLUSIONS

We have examined the dehydration and rehydration process of the recently synthesized dicarboxylate compounds $[Ln(H_2O)]_2[O_2C(CH_2)_2CO_2]_3 \cdot H_2O$ and $[Ln(H_2O)]_2[O_2C(CH_2)_3CO_2]_3 \cdot 4H_2O$ (Ln = Y, Eu, Gd). The thermal behavior of these compounds investigated by using thermogravimetric analysis and thermodiffractometry measurements shows a significant difference between the succinate and the glutarate compounds. In the latter, the water

molecules are removed at temperatures below 80°C whereas a continuous loss of water is observed for rare-earth succinate in the temperature range 25–320°C. In addition, the change in lifetime of the $^5D_0$ state of Eu^{3+} with temperature has been shown to be sensitive to the water content in the glutarate but not the succinate. In this technique, the Eu^{3+} ion acts as a probe to detect the dehydration and rehydration processes since the lifetime of the $^5D_0$ state is determined by the local surroundings. The change in lifetime in the glutarate is therefore directly correlated to the amount of water present in the channels. Similar effects have been reported previously for the dehydration and rehydration of coordination compounds (11), silica gels (12), and ion-exchange resins (13). The present findings indicate that this could be a powerful tool for the study of adsorption and desorption phenomena in zeolites.

ACKNOWLEDGMENTS

The authors thank C. D. Flint for the access to the spectroscopic equipment at the Chemistry Department of Birkbeck College, University of London, and E. Antic-Fidancev for her assistance in measuring the emission spectra at the Laboratoire de Chimie Métallurgique et Spectroscopie des Terres Rares, Meudon. E.S. and T.L. thank the CNRS for a travel grant. A.K.C. acknowledges the Région d'Ile-de-France and the Fondation de l'Ecole Normale Supérieure for a Chaire Internationale de Recherche Blaise Pascal.

REFERENCES

1. F. J. Berry, J. F. Marco, and A. T. Steel, *J. Alloys Comp.* **194,** 167 (1993).
2. S. Aceman, N. Lahav, and S. Yariv, *J. Thermal Anal.* **50,** 241 (1997).
3. K. Stahl and R. Thomasson, *Zeolites* **14,** 12 (1994).
4. F. Serpaggi and G. Férey, *J. Mater. Chem.* **8,** 2737 (1998).
5. JCPDS File No. 42–1121.
6. F. Serpaggi and G. Férey, *J. Mater. Chem.* **8,** 2749 (1998).
7. M. Bettinelli and C. D. Flint, *J. Phys. Condens. Matter* **3,** 4433 (1991).
8. T. Luxbacher, H. P. Fritzer, and C. D. Flint, *Spectrochim. Acta A* **54,** 2027 (1998).
9. T. Luxbacher, unpublished results.
10. J. L. Kropp and W. L. Dawson, *J. Chem. Phys.* **45,** 2419 (1966).
11. W. DeW. Horrocks, Jr., and D. R. Sudnick, *J. Amer. Chem. Soc.* **101,** 334 (1979).
12. A. Piazza, A. Bouajaj, M. Ferrari, M. Montagna, R. Campostrini, and G. Carturan, *J. Physique IV* **C4,** 569 (1994).
13. Y. Takahashi, T. Kimura, Y. Kato, Y. Minai, and T. Tominaga, *Chem. Comm.* 223 (1997).